Journal of Neural Engineering

PAPER • OPEN ACCESS

Synergic practice with a body-machine interface: implications for individual and collective motor learning

To cite this article: Amy Bellitto *et al* 2025 *J. Neural Eng.* **22** 046036

Journal of Neural Engineering

CrossMark

OPEN ACCESS

RECEIVED
17 March 2025

REVISED
7 July 2025

ACCEPTED FOR PUBLICATION
11 July 2025

PUBLISHED
4 August 2025

PAPER

Synergic practice with a body-machine interface: implications for individual and collective motor learning

Amy Bellitto[1,2,3], Ferdinando A Mussa-Ivaldi[4,5], Camilla Pierella[1,6,*] and Maura Casadio[1,6]

[1] Department of Informatics, Bioengineering, Robotics and Systems Engineering, University of Genoa, Genoa, Italy
[2] Spinal Cord Unit, Santa Corona Hospital, ASL2 Savonese, Pietra Ligure, Italy
[3] Cognitive Robotics Department, Faculty of Mechanical Engineering, Delft University of Technology, Delft, The Netherlands
[4] Northwestern University, Chicago, IL, United States of America
[5] Shirley Ryan Ability Lab, Chicago, IL, United States of America
[6] Equal contribution.
[*] Author to whom any correspondence should be addressed.

E-mail: camilla.pierella@unige.it

Keywords: synergic practice, body-machine interface, motor learning

Supplementary material for this article is available online

Abstract

Objective. Body-machine interfaces (BoMIs) translate human body movements into commands for controlling external devices, such as computer cursors. This process allows researchers to study the development and refinement of inverse models, which generate motor commands necessary for achieving desired movements. Traditionally, motor learning has focused on solo practice, but recent research has shifted towards exploring dyadic tasks, where two individuals practice together. Within dyadic tasks, synergic practice—where partners collaborate toward a shared goal—has shown promise in enhancing performance and reducing stress. However, the impact of contributions of each partner within synergic practice on individual and collective learning remains underexplored. This study aims to (i) investigate how different levels of contribution during synergic practice affect both individual and collective motor learning, and (ii) assess the impact of these contribution levels on individual performance when returning to solo practice. *Approach*. Forty naïve participants underwent individual practice, dyadic synergic practice, and a final round of individual practice using a BoMI to control a cursor. Participants were classified as high or low contributors based on their participation in the cursor trajectory during dyadic practice. We analyzed how these contribution levels influenced performance, motor strategies, and internal models during and after the dyadic phase. *Main results*. During dyadic practice, high contributors maintained motor strategies similar to their initial solo performance, while low contributors showed significant deviations. After returning to solo practice, high contributors retained better task performance, whereas low contributors initially regressed but quickly improved with additional practice, eventually matching high contributors' performance levels. *Significance*. This understanding holds practical implications for optimizing dyadic practice. Our study sheds light on the influence of synergic practice on subsequent individual motor performance, contributing to a clearer understanding of its advantages and limitations for optimal implementation.

1. Introduction

A fundamental theory in motor learning revolves around the concept that the central nervous system (CNS) constructs 'internal models' during the acquisition of novel motor skills [1, 2]. These internal models manifest in two distinct types: forward and inverse. Forward models anticipate the sensory consequences of motor commands, while inverse models produce the necessary motor commands for the correct execution of the intended movement. The process of motor learning involves continuously and iteratively updating these internal models. As an individual refines his/her motor skills through practice, the CNS continuously adjusts and refines these internal models based on the feedback received from sensory inputs and the outcomes of motor actions.

Within this framework, body-machine interfaces (BoMIs) offer a means to monitor the evolution of an individual's inverse model throughout the acquisition of a novel motor skill [3], serving as a tool for exploring 'internal models' in motor learning. BoMIs are systems that utilize many degrees of freedom of the human body by mapping them into a reduced set of commands for controlling an external device, such as a wheelchair or a computer cursor [4, 5]. Their inherent design allows for the estimation of the inverse model employed by the user while learning, as well as the creation of entirely new and redundant motor tasks [6]. The latter is often a challenging endeavor since traditional motor tasks rarely require the CNS to 'begin from scratch' and explore the inherent redundancy of the task itself. BoMIs address this limitation by introducing real or virtual objects controlled with an overabundant number of body signals and building a map between the high-dimensional space of the body signals and the low-dimensional control space. As the interface maps signals from the body to the task space, the learner effectively creates an inverse of this map, translating task objectives into suitable body signals to achieve the desired goal. This process involves identifying, among many, the body configurations that will allow the user to complete the task.

Leveraging the distinct characteristics of the BoMI, a recent study [3] investigated the learning dynamics within a cohort of unimpaired individuals undergoing training with the interface. This study revealed that as participants became more skilled with the task, their inverse models gradually stabilized to a single solution. These findings, combined with results from other studies [7–9], support the internal model theory, even in the context of a novel highly redundant task learned with a BoMI.

Here we translate these concepts within a dyadic scenario. Often, motor learning is conceived as a process taking place uniquely within the confines of a single person, with less emphasis on the role of human interactions [10]. This orientation towards individual learning has left an essential aspect of our day-to-day learning experiences relatively underexplored. Only in recent years, emerging studies have started to investigate motor learning within dyadic settings [11, 12]. Dyadic practice offers a more interactive, complex, and potentially realistic context for understanding motor learning. Moreover, this approach has gained significant attraction due to its potential for practical application, as it offers increased efficiency in terms of both time and costs by training two people simultaneously [13–15]. It can be explored through various interaction modalities (such as co-active and competitive), each providing unique insights into the dyadic aspects of motor learning [11]. Among these interaction modalities, synergic practice, where partners share the same task goal and work together, has demonstrated significant potential. This type of interaction, mainly investigated under conditions of haptic feedback between users [16–18], consistently enhances task performance compared to individual practice [17–20], while also inducing lower levels of stress and anxiety compared to other interaction types, like competitive tasks [14, 21], making it a preferred and constructive training approach.

Within the internal model theory, synergic training presents a unique learning environment where mastering a shared motor task necessitates the development of both individual and collective internal models. The task depends on visual feedback and the combined motor outputs of both participants, yet the contributions of each participant do not need to be equal: one participant could complete the task independently. A crucial aspect of this process is understanding how these internal models, both individual and collective, evolve during synergic practice, and how the contribution of each participant influences these changes. To the best of our knowledge, no prior research has investigated, within the context of a redundant motor task, (i) how practicing in a dyadic synergic context influences the simultaneous individual and collective learning process and (ii) how synergic practice affects the individual internal model when reverting to performing the task alone. Moreover, the impact of each participant's contribution during synergic practice on these learning processes remains unexplored.

This study aims to: (i) characterize the dynamics of dyadic learning by exploring individual behavior and motor strategies within the dyadic context, analyzing collective performance, and investigating how both individual and collective inverse models evolve with a focus on the influence of varying or equal levels of contribution; and (ii) assess the impact of dyadic training on individual task performance, motor strategies, and internal models, particularly how different levels of contribution during dyadic practice affect these outcomes.

For these purposes, we enlisted 40 naïve participants who underwent an individual practice, a dyadic practice, and another round of individual practice with a BoMI. Similar to [22, 23], participants controlled a cursor using their upper arm movements. During individual practice, participants maintained full control over the cursor, while during dyadic practice, cursor control was shared with a second participant.

We consistently observed a high contributor and a low contributor within each dyad, rather than equal control sharing. During dyadic practice, high contributors were able to adopt an individual inverse model and a set of motor strategies that closely resembled the one formed in solo practice. In contrast, low contributors, who relied more on their partners, lost their model during dyadic practice and then faced less improvement in control accuracy than high contributors when switching back to individual practice. These results underscore how contribution levels affect individual models and motor strategies during synergic interaction, with low contribution behavior leading to no additional improvements in solo performance.

Gaining insights into these mechanisms is crucial, as dyadic interaction can boost overall performance and training efficiency, but its effects on individual learning and skill retention must be carefully evaluated.

2. Method

2.1. Participants

Forty volunteers (age 26.69 ± 2.26 y.o., 20 females, table S1 in supplementary materials) with no known history of motor or cognitive impairment and naïve to the experimental setup of the BoMI participated in the study. The experiment was conducted in accordance with the guidelines of the Declaration of Helsinki and was approved by the University Institutional Review Board (code CE DIBRIS protocol—009/2020 approved on 18/05/2020). All participants provided informed consent by signing the appropriate documentation. Participants worked in dyads, resulting in a total of 20 couples tested. To ensure a balanced representation of gender combinations, couples were organized into four categories: female–male, male–female, male–male, and female–female, with five couples in each configuration.

2.2. Experimental set-up

The experiment involved pairs of participants performing a motor task using a BoMI. Each participant was seated at a separate computer workstation and interacted with the system independently, without any verbal or visual communication with their partner.

The BoMI enabled participants to control a computer cursor through coordinated movements of their upper arms. These movements were captured in real-time by two inertial measurement units (IMUs), each worn on the upper arms, and translated into two-dimensional cursor positions on the screen. Participants completed the task under two conditions: *individual*, where each person operated a separate cursor, and *dyadic*, where both users jointly controlled a single shared cursor.

During the dyadic condition, the two computers were connected via a local area network. Motion data were exchanged using Transmission Control Protocol (TCP), allowing both users to contribute to and observe the same cursor trajectory in real-time.

The sections that follow describe the motion tracking system, the mapping between body movements and cursor control, and the procedure used to construct the individual and shared mappings.

2.2.1. Motion data acquisition

Upper-arm movements were recorded using two wireless IMUs (Movendo Technology, Genoa, Italy) worn by each participant. IMU1 was placed on the midpoint of the right upper arm, and IMU2 on the midpoint of the left upper arm (figure 1(A)). Both sensors were secured with custom elastic bands to ensure consistent placement. Each IMU sampled data at 50 Hz and integrated a triaxial accelerometer, gyroscope, and magnetometer. Orientation was estimated onboard using a 3D sensor fusion algorithm and represented as a quaternion, a four-dimensional vector. The two quaternions, one from each IMU, were concatenated to produce an eight-dimensional (8D) *individual body-motion configuration vector*:

$$\mathbf{q}_s = \begin{bmatrix} q_{s_1} & \ldots & q_{s_8} \end{bmatrix}^{\mathrm{T}} \tag{1}$$

where $s = 1, 2$ denotes the user id number within each dyad. This vector was transmitted via Bluetooth to the participant's computer for real-time processing.

2.2.2. Body-to-cursor mapping

The 8D individual body-motion configuration vector obtained from the IMUs was linearly mapped into a 2D vector specifying the position of a cursor on a computer screen. The mapping from the high-dimensional body configuration space to the lower-dimensional task space (cursor position) was defined at the beginning of the experiment and varied depending on the practice condition. During the experiment, participants performed the same task under two conditions: *individual* and *dyadic*.

In the individual condition, each participant was assigned a distinct body-to-cursor map (*individual body-to-cursor map*, $\mathbf{H}_1$ and $\mathbf{H}_2$, with $\mathbf{H}_1 \neq \mathbf{H}_2$) and had complete control of his/her computer cursor (figure 1(A)).

In the dyadic condition, participants used a common body-to-cursor map (*dyadic body-to-cursor map*, $\mathbf{H}_{12}$). In this condition, both users jointly controlled a single cursor, which was simultaneously displayed on both screens (figure 1(B)).

2.2.3. Body-to-cursor maps construction

The *individual body-to-cursor maps* used in the experiment were generated from calibration data collected prior to the study. To ensure equal difficulty across mappings, data were obtained from two individuals not involved in the main experiment. Each performed a calibration 'body dance', a self-directed and self-paced movement of the upper arms, for 60 s.

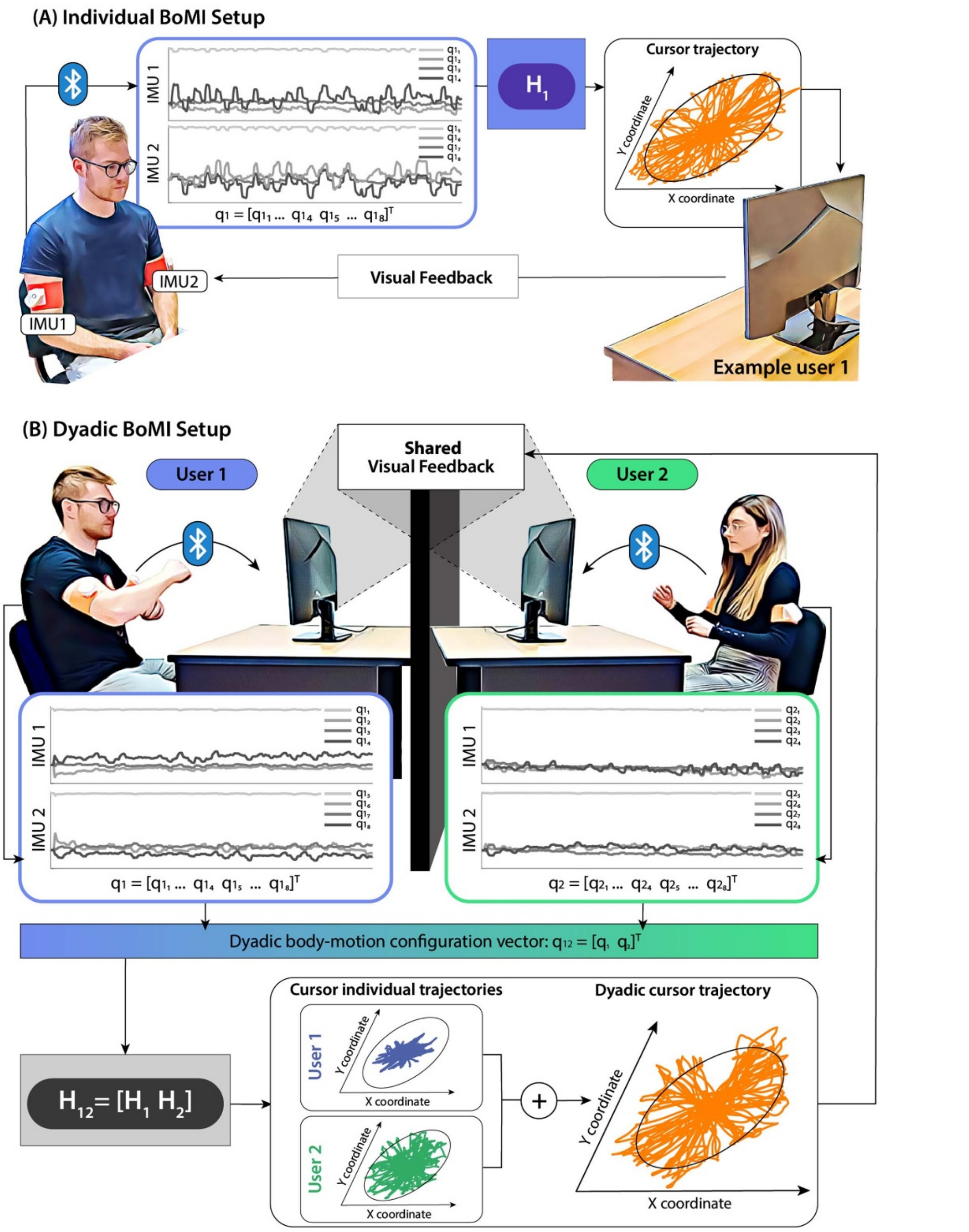

Figure 1. (A) Schematic representation of the individual body-machine interface (BoMI) setup. Two inertial measurement units (IMUs), labeled IMU1 and IMU2, are placed on the right and left upper arms to measure arm movements. The quaternion data from both IMUs is then concatenated to form the user's 'individual body-motion configuration vector' data (either $\mathbf{q}_1$ or $\mathbf{q}_2$), which is transmitted via Bluetooth (ᛒ) to a computer. This vector is then mapped using the 'individual body-to-cursor map' ($\mathbf{H}_1$ or $\mathbf{H}_2$) into a 2D vector that specifies the x and y coordinates of a cursor on the user's screen. The user has full and independent control of the cursor. (B) Schematic representation of the dyadic BoMI setup. The 'individual body-motion configuration vectors' of the two users ($\mathbf{q}_1$ and $\mathbf{q}_2$) are concatenated to form a 'dyadic body configuration vector' ($\mathbf{q}_{12}$) and then mapped, using the 'dyadic body-to-cursor map' ($\mathbf{H}_{12}$), into a 2D vector that specifies the position of the cursor shown on each user's screen. Users have shared control of the cursor and shared visual feedback.

During this period, two IMUs measured the quaternion values generated by the movement of both upper arms of one subject. Each calibration data set ($\mathbf{Q}_{\mathrm{CLB_s}}$) was organized as an $N \times M$ matrix, where M was the number of samples collected over 60 s (sampling rate = 50 Hz, $M = 3000$) and N was the number of measurement signals ($N = 8$). Following previous studies [5, 23, 24], we applied principal component analysis to extract the first two eigenvectors:

$$h_{s_1} = \left[h_{s_{1,1}} h_{s_{1,2}} \ldots h_{s_{1,8}}\right]^{\mathrm{T}} \quad (2)$$

$$h_{s_2} = \left[h_{s_{2,1}} h_{s_{2,2}} \ldots h_{s_{2,8}}\right]^{\mathrm{T}} \quad (3)$$

from each subject's dataset. These eigenvectors were then combined to build the two *individual body-to-cursor map* ($\mathbf{H}_S$):

$$\mathbf{H}_s = \begin{bmatrix} h_{s_{1,1}} & \dots & h_{s_{1,8}} \\ h_{s_{2,1}} & \dots & h_{s_{2,8}} \end{bmatrix}. \tag{4}$$

Each map, whose values are reported in equations (S1) and (S2) of the supplementary materials, was used to create a linear mapping from the body space to the cursor space for each user s:

$$\mathbf{p}_s = \mathbf{H}_s \cdot \mathbf{q}_s \tag{5}$$

where $\mathbf{p}_s$ is the 2D *individual cursor trajectory* containing respectively the x and y coordinate of the cursor:

$$\mathbf{p}_s = \begin{bmatrix} x & y \end{bmatrix}^{\mathrm{T}}. \tag{6}$$

During the dyadic practice phase, the shared body-to-cursor map ($\mathbf{H_{12}}$) was derived by concatenating the individual mappings of user 1 ($\mathbf{H_1}$) and user 2 ($\mathbf{H_2}$):

$$\begin{aligned} \mathbf{H}_{12} &= \begin{bmatrix} \mathbf{H}_1 & \mathbf{H}_2 \end{bmatrix} \\ &= \begin{bmatrix} h_{1_{1,1}} & \dots & h_{1_{1,8}} & h_{2_{1,1}} & \dots & h_{2_{1,8}} \\ h_{1_{2,1}} & \dots & h_{1_{2,8}} & h_{2_{2,1}} & \dots & h_{2_{2,8}} \end{bmatrix}. \end{aligned} \tag{7}$$

To obtain the following linear mapping:

$$\mathbf{p}_{12} = \mathbf{H}_{12} \cdot \mathbf{q}_{12} \tag{8}$$

where $\mathbf{q}_{12}$ is the 16D *dyadic body-motion configuration vector:*

$$\mathbf{q}_{12} = \begin{bmatrix} \mathbf{q}_1 & \mathbf{q}_2 \end{bmatrix}^{\mathrm{T}}. \tag{9}$$

And $\mathbf{p}_{12}$ is the 2D *dyadic cursor trajectory* containing the x and y position of the computer cursor controlled simultaneously by the two participants.

The map $\mathbf{H}_{12}$ was built as a concatenation of $\mathbf{H}_1$ and $\mathbf{H}_2$:

$$\begin{aligned} \mathbf{p}_{12} = \mathbf{H}_{12} \cdot \mathbf{q}_{12} &= \begin{bmatrix} \mathbf{H}_1 & \mathbf{H}_2 \end{bmatrix} \begin{bmatrix} \mathbf{q}_1 \\ \mathbf{q}_2 \end{bmatrix} \\ &= \mathbf{H}_1\mathbf{q}_1 + \mathbf{H}_2\mathbf{q}_2 = \mathbf{p}_1 + \mathbf{p}_2. \end{aligned} \tag{10}$$

This map configuration allowed users to share control of the cursor and, if desired, have equal control. It also enabled the computation of the individual cursor trajectories of each user ($\mathbf{p}_1$ and $\mathbf{p}_2$) during the dyadic practice phase.

2.3. Experimental protocol and task

The task consisted of a center-out reaching performed individually or synergistically. Starting from the same initial position in the center of the screen (home), participants were required to move the cursor to a peripheral target using their arm movements. Targets were presented on a blue background as white circles (1 cm in diameter). The cursor was an orange circle (0.4 cm in diameter). The distance of the peripheral targets from the center target was $r = 5$ cm. The sequence of targets presented to each participant was identical and was set at the beginning of the study. The sequence was defined to maximize participants' exploration of the workspace. To do so, we built a sequence in which targets were always presented in different positions. We divided the workspace into six arc sections (A1–A6), each subtending an angle of 60°. We then imposed two target sequence constraints: (i) no target could appear more than once in the same position within any arc section, and (ii) a target from all six arc sections had to be presented to the participant before repeating the reaching towards a target belonging to those sections.

The training protocol (figure 2) consisted of three practice phases: a 1st individual practice phase of three training blocks (T1–T3), a dyadic practice phase of three training blocks (T4–T6), and a 2nd individual practice phase of two training blocks (T7–T8). Each block consisted of a sequence of target presentations in which a peripheral target from each arc section occurred nine times (runs), for 54 center-out movements, plus the corresponding 54 out-center movements.

At the start of each block, participants were instructed to reach the external target as quickly and accurately as possible. During dyadic practice, no additional instructions were provided on coordination or control sharing, deliberately encouraging natural interaction patterns and the spontaneous emergence of role differentiation. Notably, in all blocks and trials, both individual and dyadic, the cursor disappeared after leaving the starting position and reappeared 0.5 s later, allowing assessment of whether participants relied on visual feedback or developed an internal map between body movements and cursor motion.

2.4. Data analysis

The analysis was designed to investigate how individual contributions within a synergistic dyadic context influence performance, motor strategies and both collective and individual inverse models. Since each participant in a dyad was given maps ($\mathbf{H}_1$ and $\mathbf{H}_2$) of the same difficulty, our first step was to analyze each participant's behavior during practice to assess their contribution to the dyad's cursor trajectory. After categorizing participants based on their level of contribution, we evaluated task performance, learning,

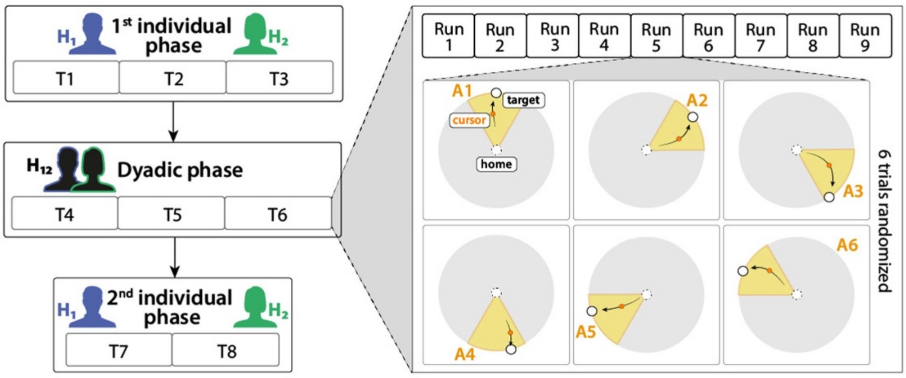

Figure 2. Schematic representation of the training protocol. The protocol is divided into three phases (1st individual phase, dyadic phase and 2nd individual phase) and each phase is divided into training blocks (T). Each block consists of nine runs of six center-out reaching trials. At each trial, the target randomly appears on one of the six possible arch sections (A1–A6).

and motor strategies to understand the following key points:

P 1 *Baseline individual practice*: to determine whether in this initial phase each participant learned to use the BoMI and establish a stable individual inverse model, a consistent set of body movements, and proficient cursor control (T1 vs. T3).

P 2 *Dyadic practice*: to determine whether in this dyadic phase the participant learned to use the collective BoMI, evaluating both the changes induced by shifting from individual to shared cursor control (T3 vs. T4) and the progress and adjustments within the dyadic practice (T4 vs. T6).

P 3 *Individual practice after dyadic practice*: to investigate wash-out of dyadic practice on the subsequent individual practice, assessing the immediate (T6 vs. T7 and T3 vs. T7) and delayed impact of dyadic practice (T7 vs. T8).

2.4.1. Individual behavior and contribution levels during dyadic practice

To analyze individual behavior during dyadic practice, we chose two parameters:

- *Contribution index*. The ratio between the length of the individual cursor trajectory of a participant and the sum of the lengths of the individual cursor trajectories of both participants. This index indicates how much the participant has contributed to the collective cursor trajectory. A Contribution Index equal to 1 means that the participant was the only contributor to the collective cursor trajectory.
- *Similarity index*. The correlation coefficient between the individual cursor trajectory of a participant and the collective cursor trajectory. It is a measure of similarity between the two trajectories (Similarity index = 1 means the two trajectories are equal).

To enhance figures' clarity, both indices will be presented as averages calculated over a moving window that includes the current trial and the 11 preceding trials.

Using the Contribution index, we categorized participants in each dyad into either the high contributor group (H.c.) or the low contributor group (L.c.) based on their relative contributions to the shared cursor trajectory. Specifically, the participant with the higher average contribution index across all trials of the dyadic phase (T4–T6) was labeled the high contributor, and the other the low contributor. Differences in contribution levels became significant by the second block of dyadic practice (T5) and remained consistent until the end (T6; see results section). This classification was then used to examine the impact of contribution on the three key points (P1, P2 and P3) outlined previously.

2.4.2. Task performance

To evaluate participants' proficiency in controlling the cursor during the center-out reaching task, the following indicators were utilized:

- *Euclidean error* at 0.5 s (in centimeters, cm). The distance between the center of the peripheral target and the center of the cursor 0.5 s after exiting the central target. We further analyzed this error by computing:
  - *Extent error* at 0.5 s (in centimeters, cm). The difference between the length of the vector connecting the cursor's starting point in the central target and the peripheral target and the length of the vector connecting the cursor's starting point in the central target and the cursor position after 0.5 s of leaving the central target.
  - *Direction error* at 0.5 s (in degrees, deg). The angle between the vector connecting the cursor's starting point in the central target to

the peripheral target, and the vector connecting the cursor's starting point in the central target to its position after 0.5 s.

- *Movement duration* (in seconds, s). The time to reach the peripheral target once the cursor exited the central target.
- *Linearity index* (adimensional). The length of the trajectory of the center-out cursor movement divided by the nominal distance between the starting and end points of that trajectory (normalized path length) minus 1. This index indicates the straightness of the cursor movement. A zero linearity index corresponds to a straight line from the central to the peripheral target.

To enhance figures' clarity, all indices will be presented as averages calculated over a moving window that includes the current trial and the 11 preceding trials.

2.4.3. Estimation and monitoring of the inverse model

To investigate the learning dynamics, we estimated, as in [3], the *inverse body-to-cursor map* (or model) used to solve the reaching problem in the individual and dyadic practice conditions. In both phases, to estimate the inverse map, we considered at each step n a sequence of r center-out reaching movements that included the *n-th* trial and the $(r-1)$ trials that preceded it. Here, we chose to consider $r = 12$ to include at least one reaching movement towards each of the six target sections [3]. Under these assumptions, at each step n, the inverse map $\mathbf{G}^{(\mathrm{n})}$ was computed by performing on:

$$\mathbf{Q}^{(n)} = \mathbf{G}^{(n)}\mathbf{U}^{(n)}. \tag{11}$$

A least squares fit:

$$\mathbf{G}^{(n)} = \mathbf{Q}^{(n)} \cdot \mathbf{U}^{(n)\mathrm{T}}\left(\mathbf{U}^{(n)} \cdot \mathbf{U}^{(n)\mathrm{T}}\right)^{-1}. \tag{12}$$

With $\mathbf{U}^{(n)}$ representing the 2D screen coordinates of the corresponding peripheral targets:

$$\mathbf{U}^{(n)} = \left[\mathbf{u}^{(n-r+1)}, \ldots, \mathbf{u}^{(n)}\right] = \begin{bmatrix} \mathrm{u}_{1,n-r+1} & \cdots & \mathrm{u}_{1,n} \\ \mathrm{u}_{2,n-r+1} & \cdots & \mathrm{u}_{2,n} \end{bmatrix}. \tag{13}$$

And $\mathbf{Q}^{(n)}$ representing the body configuration assumed by participants 0.5 s after the cursor has left the central target:

$$\mathbf{Q}^{(n)} = \left[\mathbf{q}^{(n-r+1)}, \ldots, \mathbf{q}^{(n)}\right]. \tag{14}$$

During the individual practice, each participant had her/his $\mathbf{Q}_s^{(n)}$ (s assumed value 1 or 2 depending on the map)

$$\mathbf{Q}_s^{(n)} = \begin{bmatrix} q_{s_{1,n-r+1}} & \cdots & q_{s_{1,n}} \\ \vdots & \ddots & \vdots \\ q_{s_{8,n-r+1}} & \cdots & q_{s_{8,n}} \end{bmatrix}. \tag{15}$$

During dyadic phase $\mathbf{Q}_{12}^{(n)}$ was obtained by concatenating the body configuration arrays of both subjects for each movement set n:

$$\mathbf{Q}_{12}^{(n)} = \begin{bmatrix} \mathbf{Q}_1^{(n)} & \mathbf{Q}_2^{(n)} \end{bmatrix}. \tag{16}$$

After estimating the inverse model, the learning process throughout practice was monitored by computing two metrics:

- *Inverse model temporal evolution* (ΔG), the percentage difference between consecutive estimations of the inverse model of $\mathbf{G}^{(n)}$:

$$\Delta G^{(n)} = \frac{||\mathbf{G}^{(n)} - \mathbf{G}^{(n-1)}||}{||\mathbf{G}^{(n)}||}. \tag{17}$$

  This parameter was used to assess if participants, during practice, converged to a stable representation of the inverse map both as individuals $\Delta G_s{}^{(n)}$ in the five individual training blocks (T1, T2, T3, T7 and T8) and as a dyad $\Delta G_{12}{}^{(n)}$ in the three dyadic training blocks (T4, T5 and T6).
- *Inverse model comparison with T8* (ΔG_{T8}), computed, for each participant in the dyad, as the Euclidean norm difference between each estimate $\mathbf{G}_s{}^{(n)}$ and the final estimate from the last training block (T8). This parameter was used to determine how similar each trial's inverse model estimate was to the final, most stable, and most accurate estimate of the inverse model.

2.4.4. Reorganization of motor strategies

To investigate the reorganization of body movements during practice, we considered, as in [23] and [7], the body strategies adopted by subjects to solve the center-out reaching task within the 0.5 s timeframe, when the cursor was not visible to the subject. Due to the redundancy of the interface, participants could have achieved the same 2D cursor position using either the same subset of body configurations or multiple body configurations. In earlier research involving unimpaired participants trained with a BoMI individually, it was observed that as training progressed, they increasingly relied on a stable set of body configurations to accomplish the task. Building on this finding, we aimed to explore: ($P1$) whether there would be a similar progression towards a set of stable set body configurations during the 1st individual practice; ($P2$) whether there would be modifications or adjustments to these configurations when transitioning from individual to dyadic practice, and whether there would be changes in these configurations as dyadic interaction progressed; and ($P3$) whether participants would revert to configurations similar to those used prior to dyadic practice upon returning to individual practice, or potentially adopt a different set influenced by dyadic practice.

To address these questions, we first assessed the planarity of body configurations during each practice block by calculating the percentage of variance explained by the first two principal components (2DVAF, %). This value, ranging from 0% to 100%, indicates if body movements are organized on a planar structure, with 100% representing perfect planarity. Then, we investigated the difference in the body configurations between each practice block and the last block of practice by computing the *Principal angle to T8* (PA_{T8}, deg). For each block, we considered the subspace identified by the first two PCs extracted from the body configurations in that block. We then computed the principal angle between these subspaces and the subspace at T8. PA_{T8} goes from 0° for coincident to 90° for orthogonal subspaces.

2.5. Statistical analysis

To validate our classification of participants into high and low contributors, we first conducted a mixed-design ANOVA on the Contribution index, with 'group' (H.c. vs. L.c.) as the between-subjects factor and 'training block' (T4, T5 and T6) as the within-subjects factor. The same analysis was performed for the Similarity index to examine its evolution across the dyadic phase.

A similar statistical approach was also applied to assess group differences in the metrics computed at key analysis points (P1–P3) to evaluate performance, motor strategies (2DVAF and PA_{T8}), and inverse models (ΔG and ΔG_{T8}) metrics. In the latter case, the between-subject factor was the same as the previous analysis (H.c. vs. L.c.), while the training blocks considered as the within-subjects factor varied depending on the specific point being investigated.

All statistical analyses were performed using Jamovi software (version 0.9.2.8), with a significance threshold set at $p < 0.05$. Normality was assessed with the Shapiro–Wilk test, and the Bonferroni correction was applied for multiple comparisons in post hoc analyses.

3. Results

3.1. Behavior during dyadic practice

The analysis of participants' individual behavior during dyadic practice with the BoMI (T4–T6) led to the classification of participants into two distinct groups: the high contributor group (H.c.) and the low contributor group (L.c.). In each pair, one participant consistently contributed significantly more to the task solution than the other. This distinction was independent of the map used, as 40% of high contributor participants used map 1 (H_1).

At the end of dyadic practice, the H.c. group had a Contribution index of 0.67 ± 0.12 std, while the L.c. group had an index of 0.32 ± 0.12 std (figure 3(A)). As expected, the difference between the two groups in terms of Contribution index was highly significant ($F(1, 38) = 45.1, p < 0.001$).

In addition, there were significant differences between the groups in the Similarity index (figure 3(B), $F(1, 38) = 15.2, p < 0.001$). While both groups exhibited high values for this index (Similarity index > 0.7), the high contributors consistently had higher similarity scores.

Interestingly, as practice progressed, the differences in both the Contribution and Similarity indexes became more pronounced and then stabilized. A significant group × training block interaction was observed for both parameters (Contribution index: $F(2, 76) = 21.55$; $p < 0.001$; Similarity index: $F(2, 76) = 6.67$; $p = 0.002$), with post hoc analysis indicating that the divergence between groups emerged by the second block of dyadic practice (T5) and remained significant thereafter (Post hoc: Contribution index H.c. T4–L.c. T4 $p = 0.601$; H.c. T5–L.c. T5 $p < 0.001$ and H.c. T6–L.c. T6 $p < 0.001$; Similarity index H.c. T4–L.c. T4 $p = 1.00$; H.c. T5–L.c. T5 $p < 0.001$ and H.c. T6–L.c. T6 $p = 0.001$).

Overall, as dyadic practice continued, the high contributors individual reaching trajectories became increasingly aligned with the dyadic reaching trajectories, both in terms of amplitude and profile (figure 3(C)). In contrast, low contributors exhibited shorter reaches, though with similar profiles to the dyadic reaching trajectory.

3.2. Task performance

The analysis of task performance revealed that, during the 1st individual practice session (*P*1), both high and low contributors achieved similar proficiency levels in cursor control (figure 4). Both groups improved in precision, with reduced Euclidean (figure 4(A), T1–T3: $F(1, 38) = 84.15$, $p < 0.001$), direction (figure 4(B), T1–T3: $F(1, 38) = 111.0, p < 0.001$), and extent errors (figure 4(C), T1–T3: $F(1, 38) = 16.35$, $p < 0.001$), as well as increases in speed (figure 4(D), T1–T3: $F(1, 38) = 173.85$, $p < 0.001$) and straighter trajectories (figure 4(E), T1–T3: $F(1, 38) = 127.99$, $p < 0.001$).

As participants transitioned from individual to dyadic practice (*P*2), immediate performance improvements were observed. Sharing control of the cursor resulted in reduced task Movement time (figure 4(D), T3–T4: $F(1, 38) = 16.37, p < 0.001$), as well as substantial decreases in Euclidean (figure 4(A), T3–T4: $F(1, 38) = 21.42$, $p < 0.001$), direction (figure 4(B), T3–T4: $F(1, 38) = 8.92, p < 0.001$) and extent errors (figure 4(C), T3–T4: $F(1, 38) = 49.74$, $p < 0.001$).

This initial enhancement under dyadic control was sustained throughout the entire practice phase (*P*3), with a further improvement observed solely in ¢extent error (figure 4(C), T4–T6: $F(1, 38) = 4.91$, $p = 0.03$).

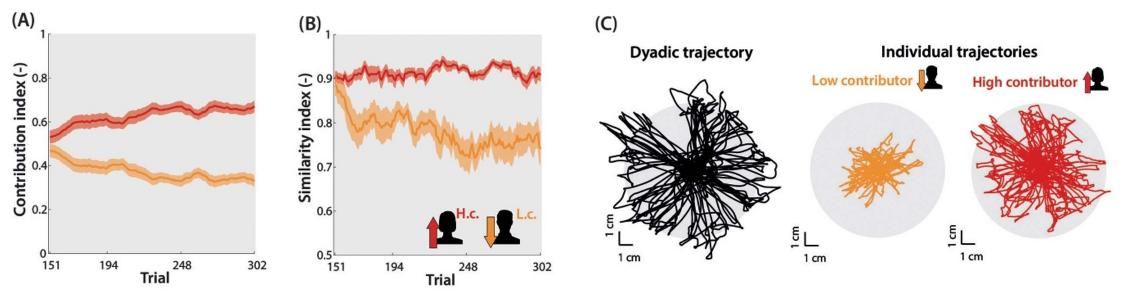

Figure 3. (A) Mean and standard error of the Contribution index (adimensional, -) during the dyadic practice. (B) Mean and standard error of the Similarity index (adimensional, -) during the dyadic practice. (C) An example of a cursor trajectory during the dyadic practice (in black) along with the estimated individual cursor trajectories of a participant identified as part of the low contributor group and another assigned to the high contributor group. In all panels, the high contributor (H.c.) and low contributor groups (L.c.) are represented by the red and orange lines, respectively. A figure displaying individual data points for each participant in panels A and B is available in the supplementary materials, figure S1.

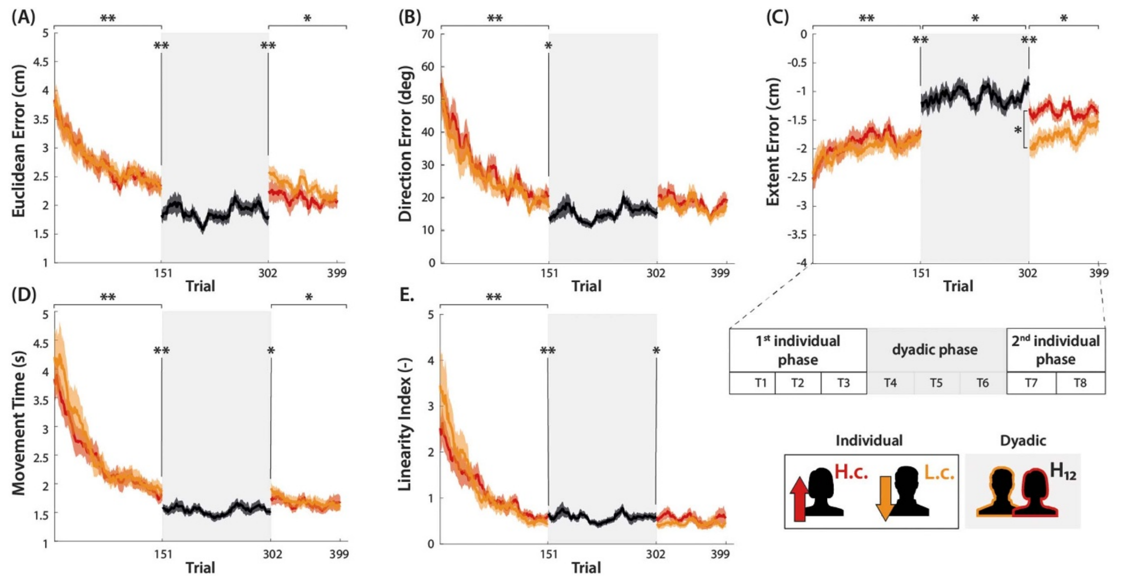

Figure 4. Mean and standard error of the cursor control parameters: (A) Euclidean error (in centimeters, cm), (B) direction error (in degrees, deg), (C) Extent error (in centimetres, cm), (D) Movement time (in seconds, s) and (E) Linearity index (adimensional, -). In all panels, red and orange lines respectively represent the results of the high contributor (H.c.) and low contributor (L.c.) groups during the two individual sessions (white background), while the black lines represent the results of the collective map (H_{12}) during the dyadic session (gray background). Horizontal brackets indicate statistically significant differences between training blocks (within-subject effects), while vertical brackets indicate significant differences between groups (between-subject effects). Statistical significance is denoted as follows: ** $p < 0.001$, * $p < 0.05$. A figure displaying individual data points for each participant is available in supplementary materials, figure S2.

Upon returning to individual practice, performance metrics of both high and low contributors largely reverted to levels seen at the end of the 1st individual session, except for the Extent error, which exhibited a significant group × training block interaction (figure 4(C), T3–T7: $F(1,38) = 12.93$, $p < 0.001$). Low contributors exhibited Extent errors comparable to, or even slightly higher than, those recorded at the end of the 1st individual practice. In contrast, high contributors showed a significant improvement in Extent error (Post hoc T3 H.c.–T7 H.c.: $p = 0.004$). However, as the 2nd individual practice progressed, the low contributor group rapidly recovered from their initially higher extent errors, achieving levels comparable to those of the high contributor group (figure 4(C)). Throughout this phase, both groups continued to improve their cursor control, as evidenced by reductions in Euclidean error (figure 4(A), T7–T8: $F(1, 38) = 5.38$, $p = 0.026$), Extent Error (figure 4(E), T7-T8: $F(1, 38) = 8.57$, $p = 0.006$), and Movement time (figure 4(D), T7–T8: $F(1, 38) = 8.49$, $p = 0.006$). No improvement was observed in terms of direction error (figure 4(B)) and Linearity index (figure 4(E)).

3.3. Individual and collective inverse model evolution

The analysis of the inverse individual model in the 1st individual session ($P1$) revealed that both high and low contributors achieved a more stable individual inverse model by the end of the session (figure 5(B), T1–T3: $F(1, 38) = 89.94$, $p < 0.001$), converging towards the model attained by the end of the entire

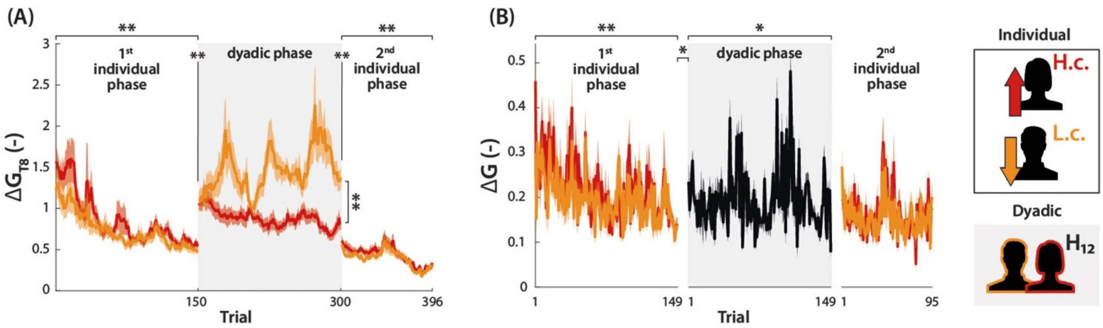

Figure 5. (A) Mean and standard error of the inverse model comparison with T8 (ΔG_{T8}, adimensional, -). (B) Mean and standard error of the inverse model temporal evolution (ΔG, adimensional, -). In both panels, red and orange lines respectively represent the results of the high contributor (H.c.) and low contributor (L.c.) groups during the two individual phases (white background), while the black lines represent the results of the dyadic map (H_{12}) during the dyadic session (gray background). Horizontal brackets indicate statistically significant differences between training blocks (within-subject effects), while vertical brackets indicate significant differences between groups (between-subject effects). Statistical significance is denoted as follows: ** $p < 0.001$, * $p < 0.05$. A figure displaying individual data points for each participant is available in supplementary materials, figure S3.

training at T8 (figure 5(A), T1–T3: $F(1, 38) = 72.54$, $p < 0.001$).

Transitioning from individual to dyadic practice (*P*2) led to a sudden shift in the individual inverse models used by both groups, causing them to deviate from the model established at T8 (figure 5(A), T3–T4: $F(1,38) = 65.98$, $p < 0.001$). This transition resulted in the initial adoption of a collective inverse model that exhibited higher ΔG values compared to the individual models employed by both groups at the end of the 1st individual phase (figure 5(B), T3–T4: $F(1, 38) = 22.64$, $p < 0.001$).

As dyadic practice progressed (*P*3), changes were observed in both individual and collective inverse models. Although both groups started this phase with similar modifications in their individual models, their trends evolved in distinct directions (figure 5(A)). The high contributor group's individual inverse model gradually and steadily converged towards the inverse model established at T8, while the low contributor group's individual inverse model showed high variability during practice and diverged significantly (Post hoc: T6 L.c.–T6 H.c. $p < 0.001$) from the inverse model established at T8. This difference between groups was significant by the end of dyadic practice (Post hoc: T6 L.c.–T6 H.c. $p < 0.001$). Despite the divergent trends in individual inverse models, the collective inverse model, though variable throughout the practice phase, became significantly more stable by the end of practice compared to its initial state (figure 5(B), T4–T6: $F(1, 38) = 11.7$, $p = 0.002$).

Returning to individual practice caused participants in both groups to revert to inverse models similar to those used at T8, rather than continuing with the model formed during dyadic practice (figure 5(A)). Additionally, there were no significant changes in the stability of the individual models in either group when compared to the stability observed at the end of the first individual session (figure 5(B)). Notably, as the 2nd individual practice continued, both groups' individual inverse models progressively converged toward the model formed by the end of T8, indicating further learning (figure 5(A), T7-T8: $F(1, 38) = 118.41$, $p < 0.001$).

3.4. Reorganization of body movements

The analysis of the 2DVAF and PA_{T8} parameters revealed that, by the end of the 1st individual practice (*P*1), both high and low contributors adopted body configurations that resulted in highly planar input data for the BoMI. This planarity increased with continued practice, reflecting the inherently two-dimensional and planar nature of the task (figure 6(A), T1–T3: $F(1, 38) = 13.79$, $p < 0.001$). By the end of the 1st individual training (T3), the level of planarity not only increased but also more closely resembled that observed at T8 than at the start of training (figure 6(B), T1–T3: $F(1, 38) = 15.24$, $p < 0.001$).

Upon transitioning to dyadic practice (*P*2), no significant differences were found in the planarity of the body configurations used by either group (figure 6(A)). However, both groups began to use motor strategies that were notably different (figure 6(B), T3–T4: $F(1, 38) = 15.21$, $p < 0.001$).

As dyadic practice progressed (*P*3), a trend of divergence emerged between groups. Low contributors gradually adopted body configurations that were slightly more planar but diverged from those used at T8, indicating reduced movement, which resulted in decreased variability in their movement data. In contrast, high contributors showed a slight decrease in planarity while converging towards the motor strategies used at T8. By the end of the dyadic training, the difference between groups was not statistically significant in terms of planarity (2DVAF) but was notable and significant in terms of changes in motor strategies, i.e. PA_{T8} (Post hoc T6 H.c.–T6 L.c.: $p = 0.003$).

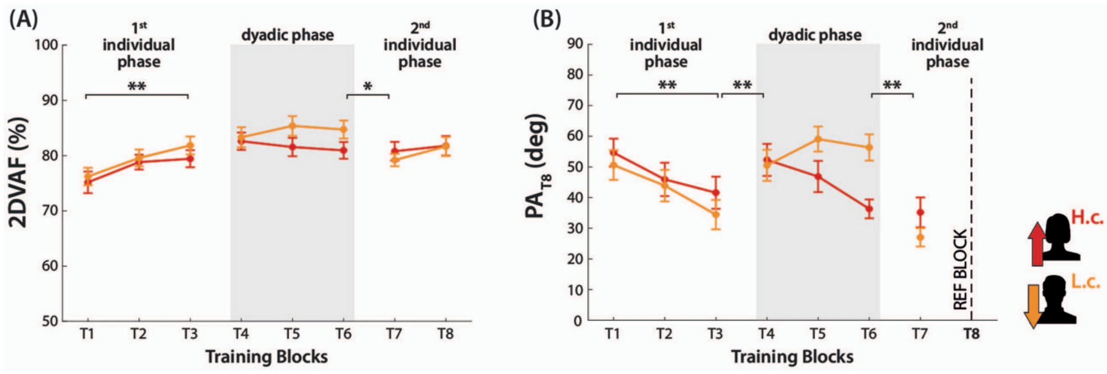

Figure 6. (A) Mean and standard error of the percentage of variance explained by the first two principal components (2DVAF, in percentage, %) extracted from the body configurations during each training block. (B) Mean and standard error of the principal angle to T8 (PA_{T8}, in degrees, deg) extracted from the body configurations during each training block. In both panels, red and orange lines respectively represent the results of the high contributor (H.c.) and low contributor (L.c.) groups. White background is used to indicate the individual phases, while a gray background is used for the dyadic phase. Horizontal brackets indicate statistically significant differences between training blocks (within-subject effects). Statistical significance is denoted as follows: ** $p < 0.001$, * $p < 0.05$. A figure displaying individual data points for each participant is available in supplementary materials, figure S4.

Returning to individual practice affected the body configurations only in the low contributor group. Post hoc analysis revealed that low contributors used significantly different body configurations compared to those at the end of dyadic practice (Post hoc T6 L.c.–T7 L.c.: $p < 0.001$), reverting to values comparable to those at the end of the 1st individual session. As a result, the differences between groups in 2DVAF and PA_{T8} values observed earlier were no longer present at T7. As the 2nd individual practice continued, neither group showed further changes in the planarity of their body configurations (figure 6(A)).

4. Discussion

In recent years, motor learning research has increasingly highlighted the benefits of dyadic training, which enhances efficiency by involving two individuals simultaneously, reducing time and resource costs. Among dyadic approaches, synergic practice has shown considerable promise. Research consistently demonstrates that synergic practice—encompassing various interaction modalities and less redundant tasks—can enhance task performance and lead to superior motor learning outcomes compared to solo training [12, 19, 25–27]. Studies on dyadic synergic training using hand-held end-effector manipulators or haptic devices in tasks such as cursor movement toward dynamic [19, 25] or static [26] targets, trajectory following [8], and pole coordination [27] have reported significantly higher performance levels than solo training. Ganesh *et al* [19], Mireles *et al* [28] and Batson *et al* [25] also discovered that synergic training markedly improved individual motor learning, with better pre-to-post-test performance. Moreover, synergic practice has been shown to lower stress and anxiety levels compared to other dyadic modalities [14] and to be more motivating and less pressure-inducing [21, 29, 30]. Despite these benefits, the dynamics of individual and collective learning within dyadic synergic contexts, especially during novel redundant motor tasks, remain unexplored.

This study addresses this gap by examining (i) how different levels of contribution during synergic practice affect both individual and collective learning and (ii) the impact of these varying contribution levels on individual performance.

In our study, participants engaged in dyadic synergic practice without being informed of the collaborative nature of the task or given any instructions on how to coordinate their actions. Under these unconstrained conditions, individuals did not contribute equally. Instead, two distinct groups were identified: high contributors and low contributors. Within each dyad, one participant consistently exhibited a higher level of contribution, performing movements that were highly similar to the collective movements in both amplitude and profile. This finding challenges the assumption that synergic practice inherently involves equal participation from both individuals.

To understand the reasons behind these differing contribution levels, we assessed individual task performance, inverse maps, and motor strategies prior to starting dyadic practice. Consistent with previous research [7, 22–24], practice led to notable improvements in performance metrics with participants refining their individual inverse maps and employing more stable body strategies [3]. Contrary to our expectations, there were no significant differences between high and low contributors at the end of the initial individual practice session. This suggests that the variability in contributions was not due to differences in expertise or learning, prompting us to consider other potential factors.

Interpersonal dynamics may be a key factor. It is plausible that the high contributor participant shaped the task's direction and influenced their partner's involvement. Research has shown that individuals that are more dominant in behavior often drive task execution and impact their partners' contributions through their influence [7]. Strategic behavior could also be a factor. Participants might have adjusted their strategies to minimize their effort. Studies on motor control suggest that individuals often optimize their efforts to conserve energy [31]. Thus, a participant may have relied more on their partner's contributions to reduce their physical exertion, leading to an imbalance in contributions. Furthermore, adaptive strategies might influence contributions. Individuals vary in how they integrate feedback and adapt their strategies [32]. A participant who employs more effective adaptive strategies and learns quickly from feedback might contribute more, whereas less effective adaptation could result in lower contributions.

Although the exact reasons for the differences in contribution remain speculative, our findings align with existing literature on the benefits of synergic practice for enhancing performance. They also clearly illustrate that varying levels of contribution significantly impact the adoption of individual inverse maps and motor strategies. During dyadic practice, high controbutors' inverse maps and body strategies gradually returned to their initial values, suggesting that their consistent contributions were beneficial in maintaining their original expertise. In contrast, low contributors' inverse maps and body strategies diverged more substantially, indicating that their reduced engagement led to more significant changes in their strategies and movements.

To assess the effects of dyadic practice on individual performance, we analyzed the final solo practice session. Participants who contributed more during dyadic practice showed improvements in Extent error that were not observed in low contributors, whose performance reverted to levels comparable to those before dyadic practice. However, low contributors demonstrated a rapid ability to achieve similar Extent error values as high contributors with minimal additional solo practice, indicating that they could quickly adjust their approach with further practice. Notably, improvements were observed only in Extent error—where contributions from both participants could effectively combine—while direction error remained unaffected. This suggests that the task structure allowed participants to achieve the same goal with reduced individual effort. The fact that both high and low contributors reverted to similar body strategies and inverse models as before dyadic practice further supports the conclusion that the impact of dyadic practice on individual performance was relatively short-lived.

These findings highlight an important nuance: while dyadic training may temporarily disrupt internal model retention—particularly in participants who contribute less—this does not appear to hinder long-term performance. Low contributors were able to rapidly regain task proficiency and re-converge toward stable internal models during subsequent solo practice. These observations suggest that the impact of shared control on internal representations is temporary, and that individual motor learning can recover quickly even after reduced engagement during dyadic practice.

5. Conclusion

Overall, our findings confirm that synergic training enhances performance, with dyads adopting, in function of their behavior, either a similar or a distinct individual internal model compared to the one they originally formed alone. This study provides critical insights into how individuals naturally engage in redundant synergic tasks and offers a deeper understanding of their influence on performance and internal model adaptation.

Significantly, our results reveal that while dyadic practice led to immediate improvements, these did not result in lasting changes when participants returned to solo practice. The fact that low contributors quickly regained their performance during the final individual phase suggests that dyadic training may transiently affect internal model retention, but not long-term performance. This highlights the need to structure shared practice in a way that supports individual consolidation, particularly for less engaged participants.

Conducted in young, unimpaired adults, this study offers initial insights on how the CNS adapts in shared-control contexts, contributing to the broader understanding of neural control and motor learning. While our findings are grounded in this specific population, they may offer valuable insights for rehabilitation and aging populations.

In particular, the use of a BoMI to support motor learning in a shared-control setting may be especially beneficial in contexts where individuals experience reduced mobility, endurance, or motivation. A key feature of our approach is that different body-to-cursor maps can be assigned to each participant, enabling individuals with varying motor abilities to practice together. This opens promising avenues for dyads composed of, for instance, a patient and a therapist, or two patients with different levels of impairment. The map configuration can be tuned to preserve task symmetry at the interface level, even if one participant has a limited motor repertoire. In this way, shared practice may promote engagement, facilitate observational learning, and ultimately support motor recovery.

Moreover, our observation that low contributors—those less engaged during dyadic practice—were still able to rapidly recover individual performance suggests that internal model adaptation can still occur even after limited engagement during shared control, as long as solo practice is resumed. This finding has practical relevance for the design of assistive protocols that alternate between active and assisted control, potentially benefiting users with limited voluntary movement.

Nonetheless, it remains essential to determine whether these dynamics hold in populations with neurological or age-related impairments, where adaptability, fatigue, and engagement may follow different patterns. Future studies should explore how personalized mappings and shared-control configurations can be adapted to optimize coordination, role emergence, and learning outcomes in clinical settings.

Data availability statement

The data cannot be made publicly available upon publication due to legal restrictions preventing unrestricted public distribution. The data that support the findings of this study are available upon reasonable request from the authors.

Funding

This work was funded by the Italian Ministry of Research, under the complementary actions to the National Recovery and Resilience Plan (NRRP) 'Fit4MedRob-Fit for Medical Robotics' Grant (# PNC0000007).

ORCID iDs

Amy Bellitto 0000-0002-5085-6689
Camilla Pierella 0000-0002-8108-9363
Maura Casadio 0000-0003-2338-8995

References

[1] Wolpert D M, Ghahramani Z and Jordan M 1979 An internal model for sensorimotor integration *Science* **269** 1880–2

[2] Wagner M J and Smith M A 2008 Shared internal models for feedforward and feedback control *J. Neurosci.* **28** 10663–73

[3] Pierella C, Casadio M, Mussa-Ivaldi F A, Solla S A and Haith A M 2019 The dynamics of motor learning through the formation of internal models *PLoS Comput. Biol.* **15** 1–25

[4] Pierella C *et al* 2014 Body machine interfaces for neuromotor rehabilitation: a case study 2014 *36th Annual Int. Conf. IEEE Engineering in Medicine and Biology Society* (*EMBC 2014*) pp 397–401

[5] Farshchiansadegh A *et al* 2014 A body machine interface based on inertial sensors *2014 36th Annual Int. Conf. IEEE Engineering in Medicine and Biology Society* (*EMBC 2014*) pp 6120–4

[6] Casadio M, Ranganathan R and Mussa-Ivaldi F A 2012 The body-machine interface: a new perspective on an old theme *J. Mot. Behav.* **44** 419–33

[7] Casadio M and Mussa-Ivaldi F A 2012 Reorganization of motor function and space representation in body machine interfaces *Proc. IEEE RAS and EMBS Int. Conf. on Biomedical Robotics and Biomechatronics* pp 326–31

[8] Liu X, Mosier K M, Mussa-Ivaldi F A, Casadio M and Scheidt R A 2011 Reorganization of finger coordination patterns during adaptation to rotation and scaling of a newly learned sensorimotor transformation *J. Neurophysiol.* **105** 454–73

[9] Mosier K M, Scheidt R A, Acosta S and Mussa-Ivaldi F A 2005 Remapping hand movements in a novel geometrical environment *J. Neurophysiol.* **94** 4362–72

[10] Kostrubiec V, Huys R and Zanone P G 2018 Joint dyadic action: error correction by two persons works better than by one alone *Hum. Mov. Sci.* **61** 1–18

[11] Küçüktabak E B, Kim S J, Wen Y, Lynch K and Pons J L 2021 Human-machine-human interaction in motor control and rehabilitation: a review *J. Neuroeng. Rehabil.* **18** 1–18

[12] Kager S *et al* 2019 The effect of skill level matching in dyadic interaction on learning of a tracing task *IEEE Int. Conf. Rehabilitation Robotics* vol 2019 pp 824–9

[13] Shea C H, Whltacre C and Wulf G 1999 Enhancing training efficiency and effectiveness through the use of dyad training *J. Mot. Behav.* **31** 119–25

[14] Abbott E F, Laack T A, Licatino L K, Wood-Wentz C M, Warner P A, Torsher L C, Newman J S and Rieck K M 2021 Comparison of dyad versus individual simulation-based training on stress, anxiety, cognitive load, and performance: a randomized controlled trial *BMC Med. Educ.* **21** 1–10

[15] McNevin N H, Wulf G and Carlson C 2000 Effects of attentional focus, self-control, and dyad training on motor learning: implications for physical rehabilitation *Phys. Ther.* **80** 373–85

[16] Kim S J, Wen Y, Kucuktabak E B, Zhan S, Lynch K, Hargrove L, Perreault E J and Pons J L 2021 A framework for dyadic physical interaction studies during ankle motor tasks *IEEE Robot. Autom. Lett.* **6** 6876–83

[17] Kropivšek Leskovar R, Čamernik J and Petrič T 2020 Dyadic human-human interactions in reaching tasks: Fitts' law for two *Mech. Mach. Theory* **84** 199–207

[18] Kim S J, Wen Y, Ludvig D, Kucuktabak E B, Short M R, Lynch K, Hargrove L, Perreault E J and Pons J L 2023 Effect of dyadic haptic collaboration on ankle motor learning and task performance *IEEE Trans. Neural Syst. Rehabil. Eng.* **31** 416–25

[19] Ganesh G, Takagi A, Osu R, Yoshioka T, Kawato M and Burdet E 2014 Two is better than one: physical interactions improve motor performance in humans *Sci. Rep.* **4** 1–7

[20] De Santis D, Zenzeri J, Masia L, Squeri V and Morasso P 2014 Human-human physical interaction in the joint control of an underactuated virtual object *2014 36th Annual Int. Conf. IEEE Engineering in Medicine and Biology Society* (EMBC 2014) pp 4407–10

[21] Gorsic M, Cikajlo I, Javh M, Goljar N and Novak D 2019 Pilot long-term evaluation of competitive and cooperative exercise games in inpatient stroke rehabilitation *IEEE Int. Conf. Rehabilitation Robotics* vol 2019-June pp 648–53

[22] Abdollahi F *et al* 2017 Body-Machine interface enables people with cervical spinal cord injury to control devices with available body movements: proof of concept *Neurorehabil. Neural. Repair* **31** 487–93

[23] Pierella C, Abdollahi F, Thorp E, Farshchiansadegh A, Pedersen J, Seáñez-González I, Mussa-Ivaldi F A and Casadio M 2017 Learning new movements after paralysis: results from a home-based study *Sci. Rep.* **7** 1–11

[24] Casadio M *et al* 2011 Body machine interface: remapping motor skills after spinal cord injury *IEEE Int. Conf. Rehabilitation Robotics* pp 405–10

[25] Batson J P *et al* 2020 Haptic coupling in dyads improves motor learning in a simple force field *Proc. Annual Int. Conf. IEEE Engineering in Medicine and Biology Society* (EMBS) vol 2020-July pp 4795–8

[26] Wang J, Chellali A and Cao C G L 2016 Haptic communication in collaborative virtual environments *Hum. Fact.* **58** 496–508

[27] Van der Wel R P R D, Knoblich G and Sebanz N 2011 Let the force be with us: dyads exploit haptic coupling for coordination *J. Exp. Psychol. Hum. Percept. Perform.* **37** 1420–31

[28] Mireles E J A, Zenzeri J, Squeri V, Morasso P and De Santis D 2017 Skill learning and skill transfer mediated by cooperative haptic interaction *IEEE Trans. Neural. Syst. Rehabil. Eng.* **25** 832–43

[29] Goršič M, Cikajlo I and Novak D 2017 Competitive and cooperative arm rehabilitation games played by a patient and unimpaired person: effects on motivation and exercise intensity *J. Neuroeng. Rehabil.* **14** 1–18

[30] Gorsic M, Tran M H and Novak D 2018 Cooperative cooking: a novel virtual environment for upper limb rehabilitation *Annu. Int. Conf. IEEE Eng. Med. Biol. Soc.* vol 2018 pp 3602–5

[31] Shadmehr R, Wise S and Schaal S 2005 The computational neurobiology of reaching and pointing—a foundation for motor learning by

[32] Meira C M and Massa M 2017 Genetic and environmental influences on perceptual-motor abilities *Psychology* **08** 1669–78